IMPACT LATERAL COMPRESSION OF THIN-WALLED CIRCULAR ALUMINUM TUBES

Takashi YOKOYAMA* and Akira SOEDA**

* Department of Mechanical Engineering, Okayama University of Science
Okayama 700-0005, Japan
** Graduate School of Engineering, Okayama University of Science
Okayama 700-0005, Japan

ABSTRACT The energy absorbing characteristics of thin-walled circular Al alloy tubes subjected to lateral compression were examined experimentally. Dynamic lateral load-deflection curves for tubes made of three Al alloys were determined with the split Hopkinson bar technique. The energy absorbing capacity to final collapse was evaluated by numerically integrating the lateral load-deflection curve for circular tubes. It is shown that the energy absorbing capacity of the Al alloy tubes depends on the material strength, the wall thickness to diameter ratio, and the deflection rate.

Keywords: *Impact lateral compression, Thin-walled circular aluminum tube, Energy absorbing capacity, Hopkinson bar, Deflection rate*

1. INTRODUCTION

The design and development of impact attenuation systems which dissipate kinetic energy in a controlled manner has received much attention in recent years, particularly in relation to the safety of vehicles of various kinds. The use of metallic structural components in such systems was reviewed by Johnson and Reid [1]. A detailed survey of the properties and characteristics of circular metal tubes under lateral compression was made by Reid [2]. Most of the work on circular tubes subjected to large lateral deformation has been done under quasi-static loading conditions (see, e.g.[3,4]).On the other hand, the dynamic lateral load-deflection curves for the mild steel and Al tubes were obtained by Reid and Reddy [5] using an existing drop-hammer facility. The dynamic response of diametrically braced metallic tubes under impact loading was investigated by Veillette and Carney [6].

The present paper is concerned with the impact lateral compression of circular tubes for estimating the energy absorbing capacity of these devices. Dynamic lateral load-deflection curves for circular tubes made of three Al alloys were accurately measured using the split Hopkinson bar technique. Static lateral compression tests on circular tubes were performed on an Instron testing machine. The energy absorbing capability to collapse or fracture was evaluated by numerically integrating the lateral load-deflection curve for circular tubes. The test results show that the energy absorbing capability is a function of material properties, tube dimensions and deflection rate.

2. SPECIMEN MATERIALS

Three Al alloys were used: 2024-T4, 6061-T6 and 7075-T6. Their nominal tensile properties are listed in Table 1. The shape and nominal dimensions of the tube specimen are given in Fig. 1. The tube specimens were machined from solid bars with a 20-mm diameter. The wall thickness t of the tube was varied from 0.5 to 1.0 mm, keeping the outer diameter unchanged (5 mm). The length L of the tube specimen was maintained constant (10 mm), since the effect of tube length on the lateral load-deflection curve is negligible for $L/D > 1$ [7] where D is the mean tube diameter.

Table 1 Nominal tensile properties of three Al alloys tested

Material	Yield strength σ_Y (MPa)	Tensile strength σ_B (MPa)	Elongation δ (%)
2024-T4 Al	415	580	17
6061-T6 Al	281	310	17
7075-T6 Al	622	672	12

Wall Thickness t (mm)	t/D
0.50	0.11
0.75	0.18
1.00	0.25

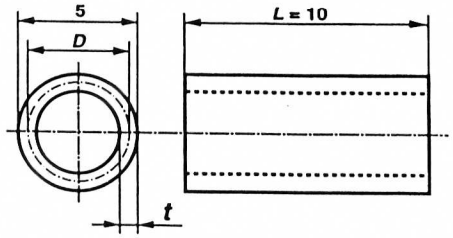

Fig. 1 Geometry of circular tube specimen

3. TEST PROCEDURE

3.1 Impact lateral compression

Figure 2 shows a schematic diagram of the standard split Hopkinson bar apparatus used for the impact lateral compression tests. The apparatus consists essentially of a very long striker bar, two Hopkinson bars (or input and output bars) and associated measurement system. The striker bar is a 1000-mm long carbon tool steel bar with a 12-mm diameter. The Hopkinson bars are made of 12-mm diameter high-carbon bearing steel rods. The tube specimen was sandwiched between the input and output bars. A loading strain pulse (ε_i) was generated in the input bar by an longitudinal impact by the striker bar fired through the barrel by compressed air released from a high-pressure reservoir, and traveled down the bar. Part of which was transmitted through the tube specimen (ε_t) and part of which was reflected back into the input bar as a tensile pulse (ε_r). The incident, reflected and transmitted strain pulses were recorded with two sets of semi-conductor strain gages bonded on the Hopkinson bars. The output signals from the strain gages were fed through a bridge circuit to a 10-bit digital storage oscilloscope, where the signals were digitized and stored at a sampling rate of 1μs/word. Further details of the test procedure can be found elsewhere [8].

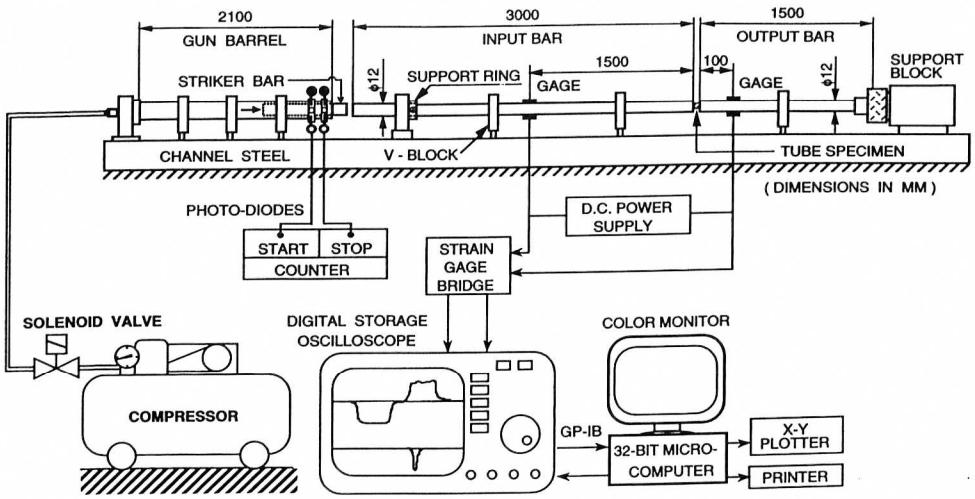

Fig. 2 Split Hopkinson bar apparatus for impact lateral compression of circular tube

3.2 Method of data analysis

From the elementary one-dimensional wave propagation theory [9], we obtain

$$\delta(t) = c_0 \int_0^t \left[\varepsilon_i(t') - \varepsilon_r(t') - \varepsilon_t(t')\right] dt' \tag{1}$$

$$\dot{\delta}(t) = c_0 \left[\varepsilon_i(t) - \varepsilon_r(t) - \varepsilon_t(t)\right] \tag{2}$$

$$P(t) = E\,A\,\varepsilon_t(t) \tag{3}$$

Here δ is the deflection of the tube, P the applied lateral load, c_0 the elastic longitudinal wave velocity, E Young's modulus, A the cross-sectional area of the Hopkinson bars; ε_i, ε_r and ε_t are incident, reflected and transmitted strain pulses; and t is the time from the start of the pulse. Equations (1) and (3) provide the deflection and the lateral load applied to the circular tube as a function of time. Eliminating time t yields the lateral load-deflection curve for the tube at the deflection rate given through Eq. (2).

4. RESULTS AND DISCUSSION

4.1 Quasi-static lateral compression tests

The quasi-static lateral compression tests were carried out with the Instron testing machine at a constant crosshead speed of 0.5 mm/min. Lubricant (MoS_2) was applied to eliminate the friction effect between the specimen surfaces and the anvils during the test.

4.2 Impact lateral compression tests

A number of impact lateral compression tests were performed on tube specimens at room temperature. Figure 3 indicates a set of typical strain-gage records from the impact lateral compression test on the 2024-T4 Al circular tube with a 0.5-mm thickness. The top trace gives an

incident strain pulse (ε_i) with compression down and a reflected strain pulse (ε_r) with tension up; the lower trace gives the strain pulse (ε_t) transmitted through the specimen. Figure 4 shows the resulting dynamic lateral load-deflection curve (solid line) and the corresponding static curve (dotted line) for the 2024-T4 Al alloy tube. In this figure, the ordinate axis denote the load per unit length of tube (or line load), and the abscissa axis indicates the deflection/mean diameter ratio. Similarly, Figure 5 indicates the static and impact lateral load-deflection curves for the 7075-T6 Al alloy tube with a 0.75-mm thickness. Note that the abrupt drops in the applied lateral load correspond to the longitudinal fracture within the tube, and the deflection rate has almost no effect on the lateral load-deflection curve before and after fractures. This is due to the very low strain-rate sensitivity of the 7075-T6 Al alloy itself.

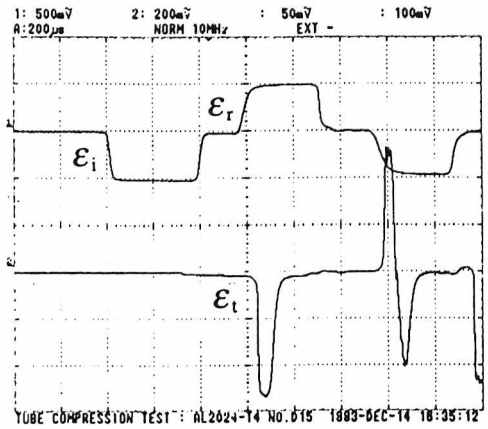

Sweep rate : 200 μs/div.
Vertical sensitivity
upper trace: 1145με/div.
lower trace: 458 με/div.

Fig. 3 Typical strain-gage records from impact lateral compression test on 2024-T4 Al alloy tube with $t = 0.5$ mm

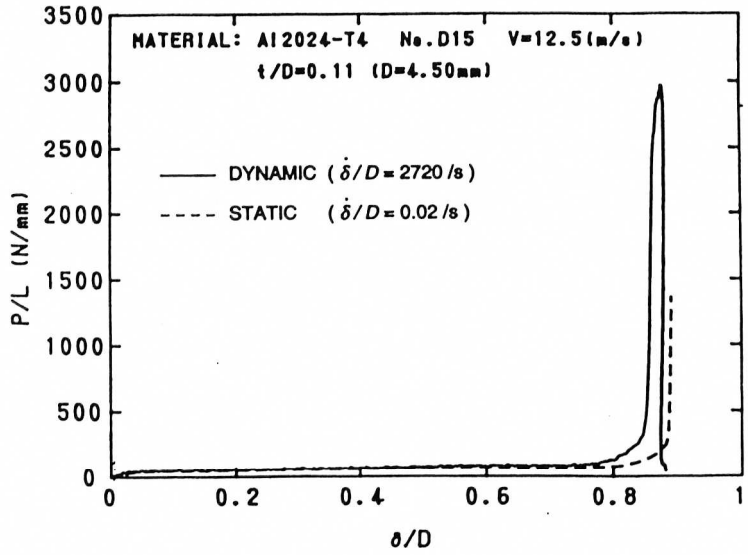

Fig. 4 Static and impact lateral load-deflection curves for 2024-T4 Al alloy tube with t =0. 5 mm

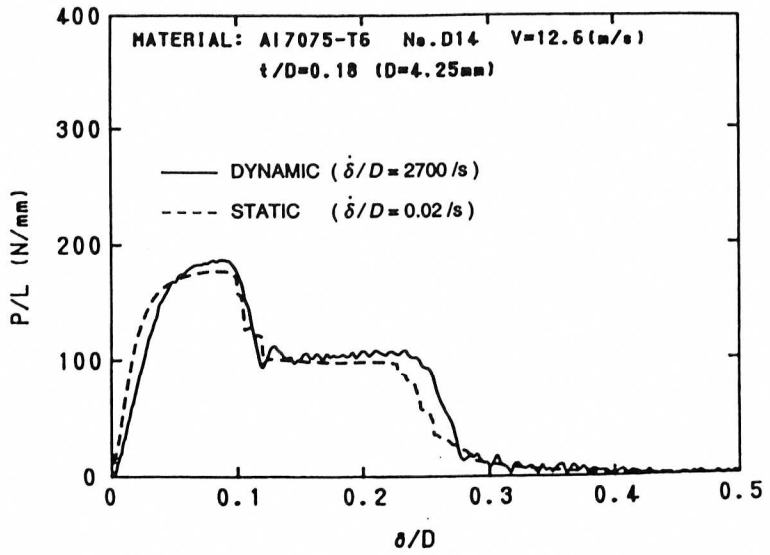

Fig. 5 Static and impact lateral load-deflection curves for 7075-T6 Al alloy tube with t =0.75 mm

Table 2 Energy absorbing capacity of three Al alloy tubes

Tube Material	Absorbing Energy W_t (MJ/m³)					
	Static			Dynamic		
	t/D = 0.11	t/D = 0.18	t/D = 0.25	t/D = 0.11	t/D = 0.18	t/D = 0.25
Al2024-T4	30.5	51.6	79.1	37.0	58.8	77.1
Al6061-T6	25.6	40.7	53.6	33.9	44.6	54.4
Al7075-T6*	11.2	13.4	14.9	11.5	13.6	13.8

* All specimens were fractured

The energy absorbing capacity of the tube was obtained by numerically integrating the lateral load-deflection curve to final collapse. Table 2 summarizes the energy absorbing capacity per unit volume of the three Al alloy tube specimens with different wall thickness ratios. It is seen that the 2024-T4 Al alloy tube possesses the highest absorbing capacity of the three Al alloy tubes. Figure 6 shows the relationship between the energy absorbing capacity per unit volume and the thickness ratio t/D. The energy absorbing capacity of all the Al alloy tubes increases with increasing wall thickness, except for the 7075-T6 Al alloy. The 7075-T6 Al alloy having the highest tensile strength exhibits the lowest absorbing capability. This is because the elongation (strain to fracture) of the 7075-T6 Al alloy is smaller than that of other two Al alloys. Note that the elongation as well as the tube thickness plays more important role than does the tensile strength to enhance the energy absorbing capacity of the thin-walled circular tube.

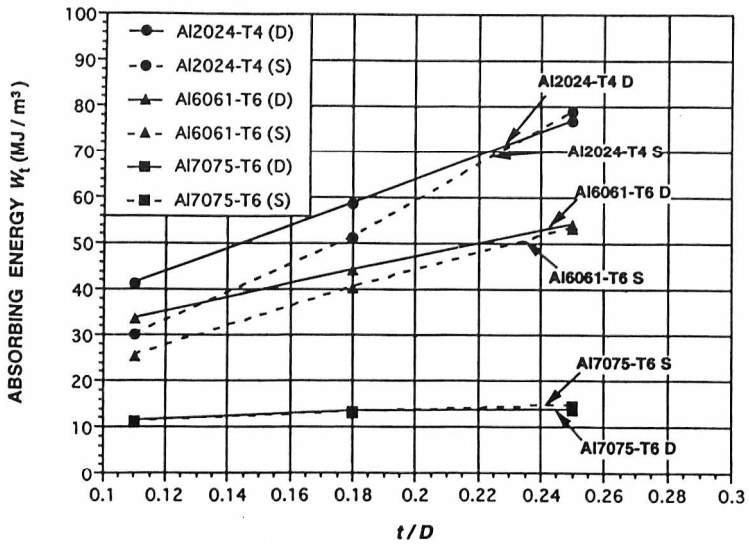

Fig. 6 Relationship between energy absorbing capacity and wall thickness of Al alloy tubes

5. CONCLUSIONS

The energy absorbing behavior of circular tubes to final collapse under lateral compression has been investigated using the split Hopkinson bar. Comparisons were made between the energy absorbing capacity of circular tubes of the three Al alloys under static and impact loading. It is found that the energy absorbing capacity of circular tubes is a function of material strength, tube dimensions and deflection rate, and that inertia effects within the tube are unimportant for the impact velocities covered in this study.

ACKNOWLEDGMENTS

The financial support of the *SHIMANO Cycle Development Center,* Sakai, is gratefully acknowledged. The test materials were supplied by *Furukawa Electric Co., Ltd.*

REFERENCES

[1] W. Johnson and S.R. Reid: *Applied Mechanics Review*, **31** (1978) 277

[2] S.R. Reid: Chapter 1 in*Structural Crashworthiness* (edited by N. Jones and T. Wierzbicki), Butterworhs, London, (1983).

[3] A.R. Watson, S.R. Reid and W. Johnson: *Int. J. Mech. Sci.* **18** (1976) 501.

[4] S.R. Reid and T.Y. Reddy: *Int. J. Solids Structures*, **14** (1978) 213.

[5] S.R. Reid and T.Y. Reddy: *Proceedings of the International Conference on Mechanical Properties of Materials at High Rates of Strain,* (edited by J. Harding), (1979) 288.

[6] J.R. Veillette and J.F. Carney, III.: *Int. J. Impact Engng*, **7**(2) (1988) 125.

[7] T.Y. Reddy and S.R. Reid: *Int. J. Solids Structures*, **16** (1980) 545.

[8] T. Yokoyama: *J. Mat Sci. Japan*, **45** (1996) 785.

[9] K.F. Graff: *Wave Motion in Elastic Solids*, (1975), Oxford University Press, London.